Regular Gaits and Optimal Velocities for Motor Proteins

R. E. Lee DeVille* and Eric Vanden-Eijnden†
*Department of Mathematics, University of Illinois at Urbana-Champaign, Urbana, Illinois; and †Courant Institute of Mathematical Sciences, New York University, New York, New York

ABSTRACT It has been observed in numerical experiments that adding a cargo to a motor protein can regularize its gait. Here we explain these results via asymptotic analysis on a general stochastic motor protein model. This analysis permits a computation of various observables (e.g., the mean velocity) of the motor protein and shows that the presence of the cargo also makes the velocity of the motor nonmonotone in certain control parameters (e.g., ATP concentration). As an example, we consider the case of a single myosin-V protein transporting a cargo and show that, at realistic concentrations of ATP, myosin-V operates in the regime which maximizes motor velocity. Our analysis also suggests an experimental regimen which can test the efficacy of any specific motor protein model to a greater degree than was heretofore possible.

INTRODUCTION

Motor proteins play a significant role in a variety of biological processes. Among other things, they drive vesicle transport, muscle contraction, and genetic transcription (1–3). There is a large body of literature on the experimental measurements (4–20) as well as the modeling (21–35) of the dynamics of such proteins.

A motor protein is made of several interacting parts: the head or motor domain, which binds to an associated filament; the tail domain, which binds to and determines the identity of the motor's cargo; and the neck or hinge region, which connects the two. The motor domain of the protein consists of some number of motor heads which detach and reattach to a filament in such a way that the mean motion of the protein is unidirectional along this filament. These detachments and reattachments are typically ATP-driven; these motors convert chemical energy to mechanical work. However, because of the scale on which motor proteins operate, and because the chemical energy is typically transferred by a single ATP molecule, a motor protein's dynamics is strongly affected by the local neighborhood of the protein. This leads naturally to considering random, or stochastic, models for the dynamics of a motor protein, using thermodynamic and chemical-kinetic considerations.

Such stochastic models have been successful in predicting observable features of motor protein dynamics (21,23,24, 27,29–37), and they have been put into a general framework in a series of articles by Fisher and Kolomeisky (27,30, 33,36). In these models, it is postulated that the motor moves randomly among several possible configurations, and the rate of switching among these states is dependent on macroscopic variables, such as ATP concentration or the force on the motor. These models have successfully predicted the statistical moments (e.g., mean and variance) of many observable quantities associated to the dynamics of several motor protein species in various parameter regimes under the application of a constant applied force.

However, when one considers the case of a motor-cargo complex in vivo, it is plausible to generalize the Fisher-Kolomeisky model to allow for the position of the cargo to change significantly while the motor head remains at one site on the filament, leading to significant variations in the force between cargo and motor. In particular, this means that the force applied to the motor can change even when the motor is stationary due to configurational changes in the tail domain of the protein, and this can lead to a significant change in the statistics of the motor dynamics. Such a generalization was first considered in Schilstra and Martin (38); the analysis of the current article pertains to the model presented there.

We will show that adding a cargo changes the dynamics of the motor-cargo complex in at least two essential ways. First, it has a strong regularizing effect on the gait of a motor protein, especially when the load is highly damped. Second, the addition of the cargo changes, in a dramatic fashion, the qualitative nature of the dependence of mean observables on various control parameters. In particular, the velocity of the motor-cargo complex as a function of ATP concentration (with everything else held fixed) is not monotone, and in fact has a local maximum, i.e., there is an optimal concentration of ATP at which the complex attains its maximum velocity, and any change in concentration decreases the average velocity of the motor. Interestingly, this velocity maximum occurs at concentrations of ATP one would typically find in the intracellular environment, i.e., in the micromolar to millimolar range. This argues that the biochemical and biomechanical characteristics of myosin-V seem to be optimized to move heavy cargos at the fastest possible velocity in the intracellular environment.

The observation that the addition of a cargo regularizes the gait of a motor-cargo complex was originally made in Schilstra and Martin (38). To the best of the authors' knowledge, the observation that any model predicts a non-

Submitted January 30, 2008, and accepted for publication May 19, 2008.

Address reprint requests to R. E. Lee DeVille, Tel.: 217-333-5601; E-mail: rdeville@uiuc.edu.

Editor: Shin'ichi Ishiwata.

0006-3495/08/09/2681/11 $2.00

doi: 10.1529/biophysj.108.130674

monotone dependence of velocity on ATP concentration is new. In this article, we describe a general technique to explain these phenomena and, in particular, compute observables as functions of the various control parameters in the models. For concreteness, our analysis focuses on the generalization of the Fisher-Kolomeisky model (33) proposed in Schilstra and Martin (38) for myosin-V, but our analysis and most of our conclusions are general and apply to other models of motor proteins as well as observables other than the velocity of the motor-cargo complex.

THEORY

We now describe the model we will consider, namely the Fisher-Kolomeisky model for motor proteins (27,30,33) and the generalization of this model due to Schilstra and Martin (38). We choose this model for concreteness, but we stress that we expect similar behavior in any model which satisfies certain general conditions (which we detail in the conclusions below).

In the Fisher-Kolomeisky class of models it is assumed that the motor protein moves along a one-dimensional track and binds at specific sites $x = \ell D$, where ℓ is an integer and D is the repeat length. To move from one binding site to an adjacent one, the protein cycles through N intermediate biochemical transitions and assumes a different configuration after each of these transitions. These steps must be visited in order, i.e., if the protein is in state S_j, then it can move forward into state S_{j+1} or backward into state S_{j-1}. To move from one binding site to the next, the motor then moves through the states $S_0, S_1, \ldots, S_{N-1}, S_0$ in order. (Periodicity is assumed; when the molecule moves forward out of state S_{N-1}, it moves into S_0.) All of the biochemical steps are reversible, and thus the molecule can walk backward by moving through these steps in reverse. Finally, the model assumes that for a fixed force on the motor, the system makes these transitions at a constant rate (i.e., there is some constant ρ so that the probability of a step in some small time Δt is $\rho \Delta t$).

Fisher and Kolomeisky showed that such a model gives a very accurate reproduction of experimental data for several motor proteins in different parameter regimes, including kinesin (30) (with $N = 4$) and myosin-V (33) (with $N = 2$) when a constant force was applied to the motor protein. We should note that this model has accurately reproduced experimental data in many parameter regimes, in particular mean and variance of motor protein velocity at forces below (27,30,33,36) and above (37) the stall force. Since this model has been so effective in modeling motor dynamics, we assume without further discussion that the Fisher-Kolomeisky model is an accurate representation of motor protein dynamics. Finally, because of the efficacy of the $N = 2$ model for myosin-V, we will concentrate on this case for the remainder of the article, but there is no theoretical restriction to applying the analysis below to higher N; see DeVille and Vanden-Eijnden (39).

Schilstra and Martin (38) extended this model to include the effect of the tail domain and its role in connecting the motor with a cargo. If the tail is modeled by a nonlinear spring (by which we mean that the force between motor and cargo is a nonlinear function of the distance between them), then the cargo relaxes toward the motor and the force on the motor is a function of time, even when the motor is stationary.

Following the Fisher-Kolomeisky framework, we further assume that the motor transition rates are of the form

$$u_k(x,y) = u_k^0 \exp\left(-\theta_k^+ \frac{F(x-y)D}{k_B T}\right),$$
$$w_k(x,y) = w_k^0 \exp\left(\theta_k^- \frac{F(x-y)D}{k_B T}\right),\ k = 0, 1, \qquad (1)$$

where we denote x as the position of the motor, y the position of the cargo, u_k as the rate to jump forward when the motor is in state S_k, and w_k as the rate to jump backward when the motor is in state S_k (see Fig. 1). If the motor's steps are given by chemical configurational changes, then these rates are just the exponential of the inverse temperature, which is consistent with the notion that the conformational changes are given by a barrier-crossing event in molecular dynamics. These choices are consistent with experiment as shown in Kolomeisky and Fisher (33). There it was also shown that for myosin-V, the $N = 2$ model replicates experimental measurements quite well, and the constants corresponding to the dynamics of the motor head were determined to be

$$\theta_0^- = -0.01, \quad \theta_0^- = 0.58, \quad \theta_1^- = 0.045, \quad \theta_1^- = 0.385,$$
$$u_0^0 = 7 \times 10^5\,\mathrm{M^{-1}\,s^{-1}}[\mathrm{ATP}], \quad u_1^0 = 12\,\mathrm{s^{-1}},$$
$$w_0^0 = 5\,\mathrm{M^{-1}\,s^{-1}}[\mathrm{ATP}], \quad w_1^0 = 6 \times 10^{-6}\,\mathrm{s^{-1}},$$
$$D = 36\,\mathrm{nm}, \quad k_B T = 4 \times 10^{-21} J. \qquad (2)$$

To generate a reasonable model of the elastic profile of the tail domain, we follow Schilstra and Martin (38), where it was assumed that the elastic profile of the tail domain corresponds to that of the coiled-coil domain of the myosin-II heavy chain. Through numerical interpolation and comparison to the data in the literature (40–42), the model for the elastic profile of the tail domain used in Schilstra and Martin (38) was

$$F(z) = az + (bz)^P, \qquad (3)$$

where

$$a = 5 \times 10^{-3}\,\mathrm{pN/nm},$$
$$b = 1.8 \times 10^{-2}\,\mathrm{pN^{0.1}/nm}, \quad P = 10. \qquad (4)$$

We discuss the effect of this choice of elastic profile further in the Concluding Remarks. We are choosing this form to be consistent with the model of Schilstra and Martin (38) and to have a concrete function for simulation. However, as we point out below, the precise details of this elastic profile are

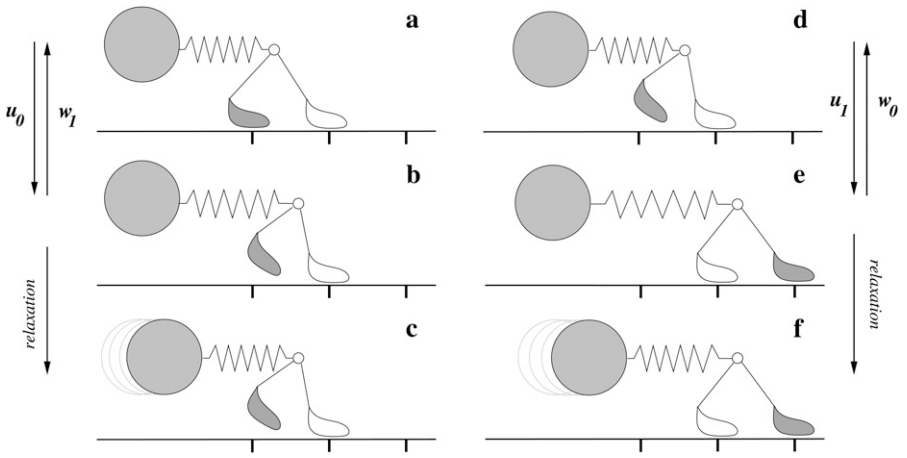

FIGURE 1 A schematic of the motor protein model we consider: if the motor progresses through steps *a–f* in order, then it has taken one forward step by the repeat length D. (We have shaded one of the motor heads so that the sequence of configurations is clear.) Note that frames *c* and *d* represent the same configuration; this state has been repeated in each column for comparison. The sequence of events in order are: switching from state S_0 to state S_1 (*a* to *b*), which corresponds to the trailing head detaching and the center of force moving by 13.5 nm; the cargo relaxing toward the motor (*b* to *c* and *d*), switching from state S_1 to S_0 (*c* and *d* to *e*), which corresponds to the loose head reattaching and the center of force moving by 22.5 nm; and the cargo again relaxing toward the motor (*e* to *f*). We note that while the $a \rightarrow b$ and $d \rightarrow e$ transitions are reversible, the relaxation stages in the dynamics are not. Once the motor heads have gone through steps $a \rightarrow f$, the entire motor-cargo complex has translated by 36 nm, and the orientation of the two heads has switched. The dynamics represented in this schematic are oversimplified; as can be seen in Fig. 2, it is not common that the motor-cargo complex makes one transition, and then waits through a relaxation period, and then makes another. It is much more common to observe the motor making many transitions back and forth between states during the cargo's relaxation toward the motor. The many back-and-forth transitions give rise to complications in the analysis and motivate the introduction of effective forces in the analysis below.

not relevant—it is sufficient that the marginal force dF/dz is large in the region in which the motor acts.

Because the rates in Eq. 1 only depend on a fraction of the total free energy, we should associate the fraction of work done in each substep with the displacements the motor undergoes in each substep. Thus the forward $S_0 \rightarrow S_1$ transition corresponds to a physical displacement by $(\theta_0^+ + \theta_1^-)D$ and the forward $S_1 \rightarrow S_0$ transition corresponds to a physical displacement by $(\theta_1^+ + \theta_0^-)D$. For the parameters above, we have that the forward $S_0 \rightarrow S_1$ step (step $a \rightarrow b$ in Fig. 1) corresponds to the motor's displacement by 13.5 nm, and the forward $S_1 \rightarrow S_0$ step (step $d \rightarrow e$ in Fig. 1) corresponds to the motor's displacement by 22.5 nm. Of course, undergoing both these forward steps leads to a total translation of $D = 36$ nm. Our schematic in Fig. 1 corresponds to the first mechanochemical pathway identified in Uemura et al. (19) for myosin-V (see Fig. 5 of (19)).

Finally, we need to model the dynamics of the cargo. Here we assume that the dynamics are overdamped, where the force on the cargo is due to that transmitted by the elastic energy of the tail domain, i.e., we have

$$\gamma \frac{dy}{dt} = F(x - y), \tag{5}$$

where γ is the friction coefficient of the cargo. The model we study in this article is now fully described by Eqs. 1–5.

This model has many parameters. We take the viewpoint in what follows that all of the parameters describing the head or tail domains of the protein are set, and the only parameters accessible to an experimenter are γ and [ATP]. The main thrust of our analysis below is to determine how the protein's dynamics depend on these two control parameters, and this can then be checked against experiments. However, while many parameters are fixed above, the analysis is not dependent on this particular choice of parameters. So, although we have myosin-V in mind specifically below, there is no theoretical obstruction to performing the analogous analysis for different motor proteins.

METHODS

We use a mixed Gillespie-differential equation method in all simulations. Given the position of the motor x, position of the cargo y, and state of the motor S_k, the rates $u_k(x, y)$, $w_k(x, y)$ can be computed from Eq. 1. The total rate of jumping is then

$$v_k(x, y) = u_k(x, y) + w_k(x, y),$$

and the time until the next jump of the motor will be exponentially distributed with mean $1/v_k(x, y)$. We sample a uniform random variable $z = U(0, 1)$ and set $\Delta t = -\log(z)/v_k(x, y)$. If this timestep Δt is below a critical threshold Δt_{max} (in this article we always chose $\Delta t_{max} = 10^{-3}$ s), then we update the position of the cargo by Δt using a discretization of Eq. 5, and push the motor forward with probability $u_k(x, y)/v_k(x, y)$ and backward with probability $w_k(x, y)/v_k(x, y)$. If the timestep determined above is larger than Δt_{max}, then we discard this jump and update the position of the cargo by timestep Δt_{max}. This is then repeated. (It is straightforward to show that this numerical method converges to the correct solution when $\Delta t_{max} \rightarrow 0$ and that there is no bias introduced by discarding the timesteps which are larger than Δt_{max}.)

We also define the transit time to be the amount of time it takes for the cargo to move one repeat length, i.e., define τ_k to be the first time when the cargo reaches kD and define the k^{th} transit time as $\tau_k - \tau_{k-1}$. To obtain statistics for these transit times, we then simulate the system as described above for long enough to capture sufficient samples of these transit times. Given the transit times, the computation of the statistics of the velocity over the repeat length, or the mean force, is straightforward.

RESULTS

This section describes a numerical study of the $N = 2$ model given in Eqs. 1–5 above. Fig. 2 shows the results of several simulations. In all frames, except Fig. 2 *d*, we have set $\gamma =$

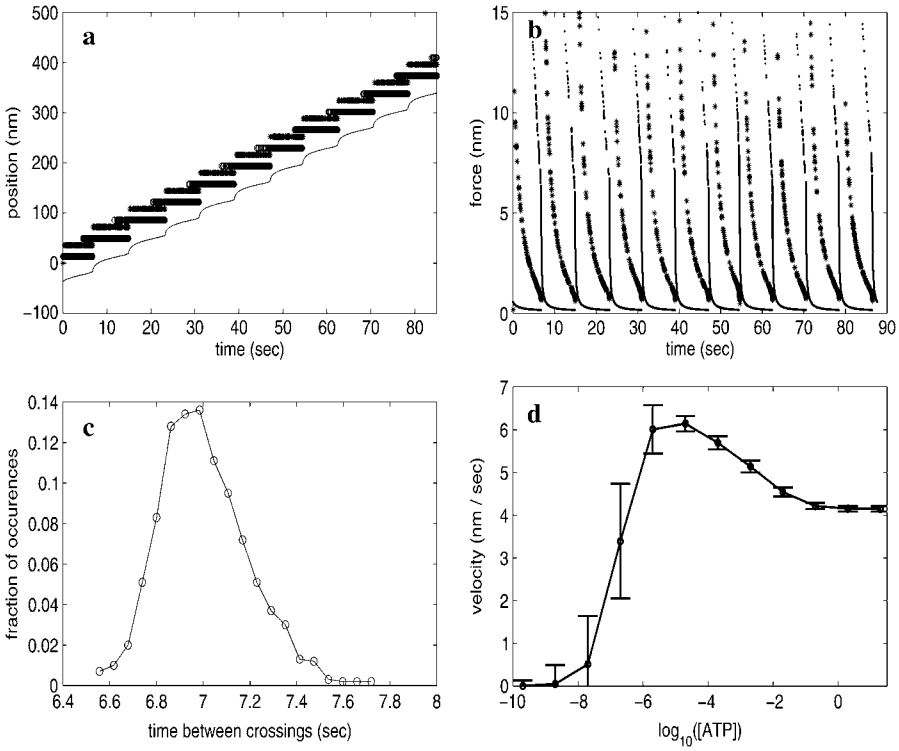

FIGURE 2 Dynamics of the motor protein model, with $N = 2$ and parameters corresponding to myosin-V as in Eq. 2. In frames *a–c* we have chosen $\gamma = 1 \times 10^{-4}$ kg/s and [ATP] = 2 mM and in frame *d* we have chosen $\gamma = 1 \times 10^{-4}$ kg/s for various values of [ATP]. In frame *a*, we plot the position of the motor and cargo as a function of time, and in frame *b* we plot the force applied to the cargo versus time. In each case we have plotted the position and force when the motor is in state S_0 with circles and in state S_1 as stars. In frame *c*, we plot a histogram of the samples of the transit time (see text for precise definition) of the cargo over one repeat length (here 36 nm). Note the axes; this measurement actually has a very small variance. In fact, for these parameters, we have the mean of the transit time as 7.00 s, with standard deviation 0.19 s, giving a coefficient of variation of 2.73%; this is a very regular process. Finally, in frame *d*, we plot the mean velocity of the motor-cargo complex for various values of [ATP] and with γ held fixed at 1×10^{-4} kg/s. Here the circles represent the mean velocity and the error bars the standard deviation. As mentioned in the text, this velocity is not a monotone function of [ATP]; there is an optimal value of [ATP] where the velocity of the complex is ~50% faster than at ATP saturation. Moreover, we see that for [ATP] sufficiently large the standard deviation of the velocity becomes quite small.

10^{-4} kg/s and [ATP] = 2 mM. In Fig. 2 *d*, we set $\gamma = 10^{-4}$ kg/s and vary [ATP] over a range. There are two remarkable features of the simulation in Fig. 2: the regularity of the motor gait and the nonmonotonicity of the motor velocity as a function of [ATP]. Let us elaborate on these two features.

Regularity

It can be seen from the simulations in Fig. 2, *a* and *b*, that the motion of the motor-cargo complex is quite regular for these parameters: the position of the cargo as a function of time is very close to a periodic motion plus a mean positive motion, and force versus time is very close to periodic. To quantify the regularity of this motion, we numerically compute the probability distribution of the transit times in Fig. 2 *c*. If the system were deterministic and periodic (i.e., perfectly reliable), then the interstepping times would be a constant and the standard deviation of this data would be zero. By way of comparison, the histogram shows that it is actually quite close to regular: we obtain a mean of 7.00 s and a standard deviation of 0.19 s, so the ratio of standard deviation to mean is $<3\%$. This verifies the visual impression from Fig. 2, *a* and *b*, that the dynamics is quite reliable.

We claim that the reasons for this regularity are generic and that such regularity should be observed for a wide variety of parameters or models (in fact, such regularity was generically observed in numerical simulations for a wide variety of parameters in (38)). We give here a short summary of the computation which shows this (the full details are in the Appendix).

The method consists of first deriving the probability that the motor jumps before the cargo reaches position y_F, if the motor is at x, and we start the system with the cargo at y_I. This is the cumulative probability distribution of the variable y_F for x and y_I fixed; we denote this function by $G(x, y_I, y_F)$. There is an associated probability distribution

$$p_{x,y_I}(y_F) = \frac{\partial}{\partial y_F} G(x, y_I, y_F),$$

and the samples of this distribution determine the (random) position of the cargo at the next jump whenever the motor is at x and the cargo starts at y_I. In general, this function $p_{x,y_I}(y_F)$ could be very spread out, which would suggest that the location of the next jump is very random. However, the crucial result of the calculations below is that the function $p_{x,y_I}(y_F)$ is very sharply concentrated near a particular value of y_F, meaning that the position of the cargo at the subsequent jump, while random, has a very small variance.

The biophysical reason that this probability distribution concentrates is straightforward: since the timescale of jumping depends on the force, as the cargo relaxes toward the motor the jumping timescale can change significantly. In fact, there is a critical y_F at which the jumping timescale goes from being much longer than the relaxation timescale of the cargo

to being much shorter than this timescale, so that the probability of a jump changes from being exponentially small to exponentially close to one in a short time. The result of this is that one will observe a regular jump at the location where these two timescales switch.

We can actually compute the variance of the cargo's position at the motor's jumping time quantitatively. The details of this computation are in the Appendix, but we summarize here. Define the relaxation timescale of the cargo to be a/γ, i.e., the ratio of the linear spring constant to the friction coefficient. If the motor is held at position x and is in state S_k, then we define y_k^R to be the position of the cargo at which the motor's jumping timescale equals the cargo's relaxation timescale, i.e., $u_k(x, y_k^R) = a/\gamma$. We further define the nondimensional temperature $\epsilon = k_B T/aD^2$ and the nondimensional force $\phi(x-y) = a^{-1}D^{-1}F(D(x-y))$. We then compute (see Eq. 17) that there are two constants $C_1, C_2 > 0$, such that whenever we are in state S_j,

$$\langle y_F \rangle = y_j^R + C_1 \epsilon/\phi'(y_j^R), \quad \langle (y_F - \langle y_F \rangle)^2 \rangle = C_2 \epsilon/\phi'(y_j^R).$$

We write the terms in this fashion to stress that the error in either of these terms is proportional to ϵ and inversely proportional to $\phi'(y_j^R)$; in particular, the variance can be made small either by decreasing ϵ or by increasing ϕ'. This correction term can be made as small as desired only by changes to the elastic profile of the tail domain. To make the motion of the protein regular, it is not necessary to modify the characteristics of the head domain, or any other environmental parameter, e.g., temperature or chemical concentrations.

In the particular case of myosin V, it is easy to see that the dominating effect is the biphasic nonlinearity in the elastic profile of the tail domain. Plugging in parameters (see the Appendix for detail) we obtain

$$\phi'(y_0^R) \approx 202; \quad \phi'(y_1^R) \approx 17.1; \quad \epsilon \approx 0.618.$$

Thus, the motor is operating in the regime where the nonlinearity in the elastic profile of the tail domain is the dominant regularizing effect.

Maximal velocity

Second, we comment on the presence of a local maximum in the velocity curve, meaning that there is an optimal concentration of ATP for the velocity of the motor-cargo complex (see Fig. 2 *d*). This effect is related to the fact that, at least for some proportion of the time, the motor is highly oscillatory between two states (as is apparent in Fig. 2, *a* and *b*). Moreover, the force, as a function of time, undergoes large instantaneous changes because the motor is jumping between subsequent sites. Thus, on the cargo timescale, the position of the motor (and thus the force felt by the cargo) is averaged over many motor sites. If the motor and cargo are in a regime where a jump forward is rare, yet increases the force significantly, then this allows the average force to be significantly changed by rare but powerful out-of-equilibrium events. We will see that this effect is exactly what allows for the counterintuitive dependence of the motor-cargo complex on various parameters and argue that this should be observed generically whenever a motor cycles through multiple configurations during a forward step.

We first want to compute the mean force felt by the cargo (it is clear from Eq. 5 that from this we can compute the mean velocity). First consider the thought experiment where we hold the cargo forever fixed at position y. The motor would then move among several sites, but we expect that after enough time the motor will settle down to its steady state, i.e., if the motor is held fixed at a given y, there is a probability distribution π_y where $\pi_y(x)$ is the probability of finding the motor at location x (or equivalently, the proportion of time the motor spends at position x is $\pi_y(x)$). From this we can compute the average force the cargo will feel when it is at position y, namely

$$f(y) = \sum_x \pi_y(x) F(x-y). \tag{6}$$

The entire system is invariant under translation by the repeat length D, so f must be a periodic function with period D. To compute the velocity of the cargo, we coarse-grain Eq. 5:

$$\gamma \frac{dy}{dt} = f(y). \tag{7}$$

Thus, instead of computing the average velocity, the correct variable is the average effective force given by γ times the average velocity. From Eq. 7, the time it takes the cargo to move one repeat length D is

$$T := \gamma \int_0^D \frac{dy}{f(y)}, \tag{8}$$

and thus the mean velocity is D/T. The mean velocity scales like γ^{-1}, so the universal quantity for γ large should be the average effective force $\gamma D/T$, and thus the velocity derived from Eq. 8 corresponds to an infinite friction limit.

In Fig. 3, we plot γ times the numerically computed mean velocity as derived above and compare it to numerical simulations. We have plotted this curve in Fig. 3 *a*. Note that it peaks for intermediate values of [ATP] with a velocity ~50% larger than that for [ATP] large or small, and is clearly nonmonotone. Since this is γ times the mean velocity of the motor-cargo complex when γ is large, for γ large but fixed this implies that the mean velocity will also peak for intermediate values of [ATP]. The most important observation here is that the theoretical maximum velocity is actually in a realistic regime for ATP concentration, being <2 mM saturation.

The solid curve in Fig. 3 is only an approximation to the real dynamics, since the analysis depends on γ being sufficiently large. In Fig. 3 *b*, we show direct numerical simulations of the model compared to the infinite friction limit and note that, first, the approximation is quite good when [ATP] is large enough for a given γ, and second, the approximations

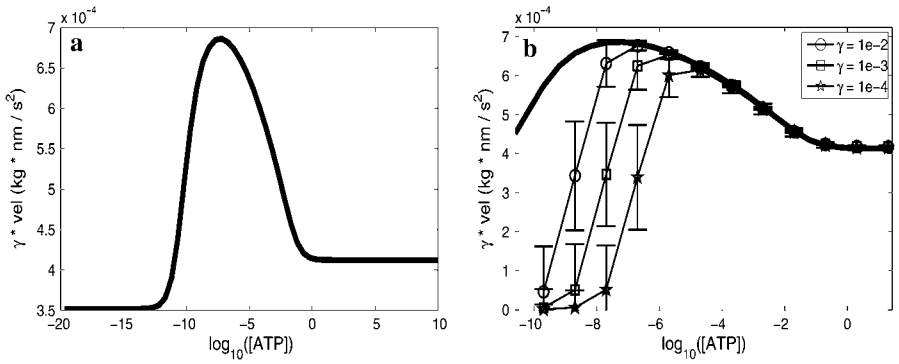

FIGURE 3 In frame *a*, we plot the theoretical mean force felt by the cargo (i.e., γ multiplied by velocity, calculated using Eqs. 6, 8, and 20) when γ is chosen sufficiently large for the steady-state analysis to be accurate. We see that there are two limits when [ATP] is chosen sufficiently large or small, but there is a intermediate range where the velocity is even larger. In frame *b*, we compare the results of simulations to the theoretical large-γ curve. We see that for any given fixed γ, the prediction is quite good for [ATP] large enough, and for fixed [ATP], the prediction gets better as γ increases. Also note that even though there is a positive limiting average force for the theoretical curve as [ATP] $\to$ 0, for a fixed finite γ, the velocity tails-off to zero if [ATP] becomes too small.

improve uniformly as γ is increased. However, for any γ fixed, if [ATP] becomes sufficiently small, the approximation breaks down and the velocity of the complex goes to zero. This makes sense: if [ATP] is too small, then the forward step out of state S_0 is never activated and we expect the complex to stall. Thus, we expect that if [ATP] is chosen so that u_0^0 becomes $<\gamma$ (see Eq. 2), then the complex stalls, i.e., stalls for

$$[\mathrm{ATP}] < \frac{\gamma}{7\times 10^5} \approx 1.43\times 10^{-6}\gamma,$$

which is (up to an order of magnitude) where the motor stalls in the direct simulations in Fig. 3 *b*. Specifically, if we choose $\gamma = 1\times 10^{-4}$ kg/s, then the approximation is very good for [ATP] ≥ 2 μM, i.e., within three decades of saturation. In summary, it seems that for a cargo with γ as large as, or $>10^{-4}$ kg/s, the parameters for myosin-V have been optimized to move at maximal velocity in the expected range of ATP concentrations.

The question which remains is this: Why should an intermediate concentration of ATP be more effective than a high or a low one? To answer this, we consider the profile of $f(y)$ for various values of [ATP] (see Fig. 4).

This force profile is not close to a constant for any concentration of ATP (and this is precisely why the constant-force model gives much different predictions). For large or small concentrations of ATP, this force profile has one large maximum, but for intermediate regimes it has two. Let us choose axes so that the motor lies in state S_0 when $x = 0$. If we choose [ATP] large, then the motor spends little time in state S_0, since both of the rates u_0 and w_0 are ATP-activated. Thus the system spends little time in any even-numbered location, so that when it goes forward, it will effectively skip all steps with state S_0 (these states are located at $x = k36$ nm for k an integer) and thus must make two steps forward at once (see Fig. 5, *a* and *b*). Similarly, when [ATP] is small, the system spends all of its time in state S_0 and thus must effectively skip the S_1 states and again switches very rapidly by two states (see Fig. 5, *e* and *f*). Thus, the system in either of these two limits is essentially acting like a $N = 1$ motor with one step per repeat length. These cases are qualitatively represented by the fact that for [ATP] small or large, the function $f(y)$ has one large bump. On the other hand, at an intermediate level of [ATP] (see Fig. 5, *c* and *d*), there are effectively two places where the motor can step forward, and two places where $f(y)$ can be relatively large. This is the nonlinearity in the tail domain coming into play: if the motor makes steps forward, even rarely, the force felt after the step forward is relatively large, and this pushes up the mean force the cargo feels (and thus pushes up the velocity). Because of the nonlinearity, the rare step forward does more work than the rare step backward, and this asymmetry is precisely what allows for such a large gain for intermediate values of [ATP].

This scheme can be carried out for any model in the framework we are considering here. The only assumption we

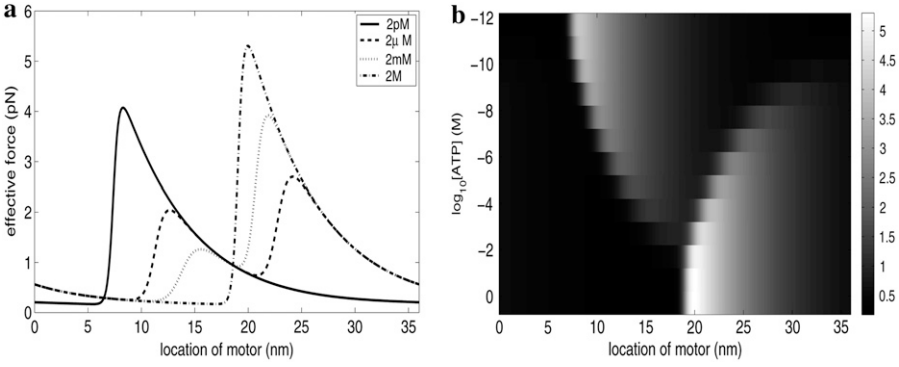

FIGURE 4 Two visualizations of the same data. Frame *a* is a series of plots of the effective force versus y for various choices of [ATP], and frame *b* is a surface plot versus y and [ATP]. This curve is single-peaked for [ATP] both very large and very small, but has a double peak for intermediate values of [ATP]. We have chosen some extreme (and unphysical) values of [ATP] for the purposes of illustration, but notice that there is a significant difference even between [ATP] = 2 mM and [ATP] = 2 μM.

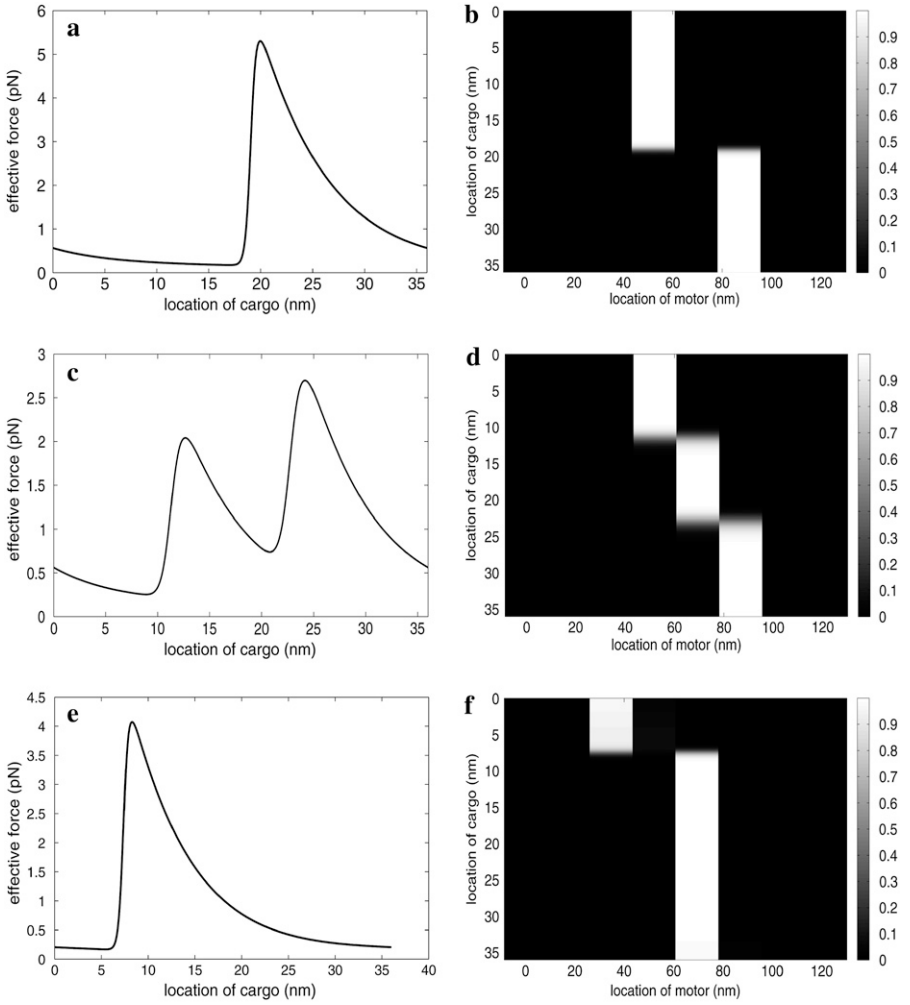

FIGURE 5 These pictures represent the calculation of the effective force versus cargo position, and the steady-state location of the motor versus cargo position, for [ATP] = 2 M (*a* and *b*), [ATP] = 2 μM (*c* and *d*), and [ATP] = 2 pM (*e* and *f*). As mentioned before, the high and low values of ATP concentration chosen here are completely unphysical, but we choose extreme values to accentuate the differences. The left frames (*a*, *c*, and *e*) here are the force-versus-position graphs as shown in Fig. 4, and in the corresponding right frames (*b*, *d*, and *f*) we show a surface plot of the steady-state motor location probability $\mu_x(y)$ for $y \in [0, 36]$nm. Not surprisingly, we see in each case that as we increase the cargo's position y, the expected location of the motor increases as well. Also, the location of the sharp increasing gradients in the force profile corresponds to the location where the motor switches from one site to the next. As explained in the text, for low and high [ATP], the motor is only allowed to use half of the sites and must effectively jump by two steps at once; whereas, for intermediate [ATP], it can use the intermediate location as well.

have used is that the cargo moves slowly enough that the motor's location is well approximated by its steady-state distribution, but as long as γ is sufficiently large, this will give an accurate measurement of the mean velocity. Whenever the tail domain has a nonlinear elastic profile, and the head undergoes intermediate conformational configurations, the effect described here can affect the velocity of the motor-cargo complex: nonequilibrium events can raise the effective average force felt by the cargo and thus the mean velocity as well.

CONCLUDING REMARKS

We have analyzed a model for motor protein dynamics and shown that there is a significant change in the dynamics of a motor protein when it is tethered to a cargo. The two differences we have concentrated on are the regularization of the motor under the addition of a heavy relaxing cargo, and the effect of nonlinearity in the elastic profile of the tail domain allowing the motor to optimize its motion in a surprising and nontrivial manner. The mechanism which drives this regularization is as follows: since the timescales on which the system jumps are functions which are very sensitive to changes in the variables (note the small denominator in the exponent in Eq. 9), the timescale corresponding to jumping can quickly go from being much longer than the cargo's relaxation timescale to much shorter. For the right parameters this can make the system jump reliably at a certain place in phase space, and this leads to regularity. This is another example of a general phenomenon, termed self-induced stochastic resonance, which frequently occurs when a system with two timescales is perturbed by a random process (43–46).

The nonlinearity in the tail domain of the protein can play a huge role in the qualitative aspects of the dynamics. The nonlinearity allows the complex to use events which push the system out of equilibrium (if only for a short time) to speed up the motion of the complex. The fact that the motor's reach exceeds its grasp is crucial to the high velocity it can achieve for intermediate concentrations of ATP. The computation of the moments shows that for any given head domain on a protein, the entire dynamics of the motor-cargo complex can be made as regular as one would wish simply by modifying the elastic profile of the tail domain only. In particular, this shows that the modifications needed to achieve this are relatively minimal and require no modification of the head's or the fil-

ament's characteristics. This could be selected simply by the protein's choosing the length and amino-acid makeup of the long tail itself. As mentioned above, the numerics seem to suggest that the parameters corresponding to myosin-V are optimal in the sense that they give a large velocity in the range of expected ATP intracellular concentration (47).

The analysis used above was in fact very general and did not use, in any crucial manner, the exact form of the model adopted here. For example, this model assumes that the cargo only moves in one dimension, but an extension of these methods to the case where the cargo is allowed to move in three dimensions would not change the analysis qualitatively: the only crucial quantity driving the process was tether extension. In addition, one could add a stochastic component to the motion of the cargo. Although this would complicate the analysis, a similar analysis incorporating this is possible; see e.g., DeVille et al. (46), where the authors consider a slow-fast system where both subsystems are stochastic. Although a specific elastic profile was chosen in Eq. 4 for concreteness, there is nothing special about the form. For example, from Eq. 17 we see that there are two ways to make the jumping times regular: if ϵ is small, or $\phi'(y_k^R)$ is large, then the variance of the jumping times will be small. While it is certainly true that the choice of biphasic elastic profile made in Eq. 4, suffices, it is by no means necessary. In fact, any elastic profile which is chosen so that its derivative is large in the region corresponding to the typical separation between motor and cargo at the jump times will give a similar regularization.

This analysis can (and in fact has been) generalized to more general motor models. In this article, the reaction rates are specified by fiat, but the general model would be to postulate that the dynamics of the motor's configuration corresponds to diffusion in some complicated potential and that the configurational changes correspond to passages past some bottlenecks in the potential. The authors have considered a motor model where the position of the motor was given by diffusion in a potential (of Brownian ratchet type) in DeVille and Vanden-Eijnden (48) and have shown that one also obtains regularity there in the correct scaling limit.

As mentioned above, the protein can achieve regularity for any head domain simply by modifying the characteristics of its tail domain. Here we discuss why such a protein would find it preferable to lie in the parameter regime which gives regular behavior; we argue that there are at least two main reasons. The first preference a motor might have toward a regular gait is in the context where a family of these proteins are strung serially along one filament (this preference was also pointed out in (38)). If the motion of these motors is quite random, this requires the density of the family to be low, otherwise the motors would likely collide and potentially cause traffic jams. It has been noted in the literature (49) that this is one main advantage of nonprocessivity for motor proteins and that densely-packed populations of motors are required to be nonprocessive. However, enforcing regularity of gait is another mechanism to allow for a dense population of motors to all use the same filament; if they move in unison, order prevails. The second preference a motor might have toward a regular gait is that at a given ATP concentration, the motor-cargo complex is more efficient at higher γ, in the sense that the mean effective force on the cargo, γv, is greater. Thus, the motor can do more work at higher γ (see the *right frame* of Fig. 3 and note that increasing γ always increases the γv-curve). This is because the cargo is moving slowly enough that the motor is allowed to sample a collection of sites, and its rare excursions into nonequilibrium locations allow the complex to place a much higher average force on the cargo. In short, what this suggests is that it is more efficient for a motor protein to carry a heavy cargo than for a family of them to separately carry light cargos, or, equivalently, it is more efficient for a population of motors to collectively act on the same heavy cargo than to break the cargo into pieces and let several motors act independently. There are many examples of collective motor protein action (1,22,49,50), one of the most notable being muscle contraction. The authors have in fact studied a model of this exact kind of collective motor protein action (39) and shown that there are some nontrivial collective effects which drive such populations. The analysis above points to the conclusion that collective action can be more efficient than independent action.

However, the observed nonmonotonicity is truly dependent on γ being large: in Fig. 3, as γ is chosen smaller, the local maximum decreases and the curve becomes more monotone. For small enough γ, the motor-cargo complex is far from the parameter regime described in this article, and the dynamics are best described by a Fisher-Kolomeisky model without the addition of the elastic profile. This is consistent with experimental data even if there were a small experimental effect due to the elastic nature of the motor-cargo connection—if γ is positive but sufficiently small, the system should act like a pure Fisher-Kolomeisky model and reproduce monotone dependence on [ATP].

Finally, we point out that the fact that the relaxing cargo can change the dynamics of the motor-cargo complex so dramatically may allow for a fuller range of experiments to be done to test a given motor protein model. The analysis above predicts how a motor-cargo complex should act in the presence of a highly damped cargo, and one could test the accuracy of the myosin-V model by comparing the velocity-[ATP] curve of Fig. 3 to experiments where, instead of holding the cargo at a constant distance from the motor as was done in the literature (5,7–9,11–13,16,18), the cargo is forced to relax toward the motor in a way which mimics the type of overdamped relaxation we would expect to see in vivo.

APPENDIX

Asymptotic analysis

We consider the most general case where $F = F(x-y)$ is a nonlinear function of the separation between motor and cargo, and there are N steps in the process describing the motor dynamics. We have

$$u_k(x,y) = u_k^0 \exp\left(-\theta_k^+ \frac{F(x-y)D}{k_B T}\right),$$
$$w_k(x,y) = w_k^0 \exp\left(\theta_k^- \frac{F(x-y)D}{k_B T}\right),$$

and we also have

$$\frac{dy}{dt} = \gamma^{-1} F(x-y).$$

We rescale by

$$x = D\hat{x}, \quad y = D\hat{y}, \quad t = B_k \hat{t}.$$

Further define $a = F'(0)$ and rescale F by

$$F(x-y) = aD\phi(\hat{x}-\hat{y}).$$

This gives (dropping hats for economy of notation)

$$u_k(x,y) = B_k u_k^0 \exp\left(-\theta_k^+ \frac{aD^2\phi(x-y)}{k_B T}\right),$$
$$w_k(x,y) = B_k w_k^0 \exp\left(\theta_k^- \frac{aD^2\phi(x-y)}{k_B T}\right),$$
$$\frac{dy}{dt} = \gamma^{-1}\phi(x-y).$$

Choose $B_k = (u_k^0)^{-1}$ for each k, finally giving

$$u_k(x,y) = \exp(-\theta_k^+ \phi(x-y)/\epsilon),$$
$$w_k(x,y) = \rho_k \exp(\theta_k^- \phi(x-y)/\epsilon), \quad \frac{dy}{dt} = \delta_k \phi(x-y), \quad (9)$$

where we have the $(2N + 1)$ nondimensional parameters

$$\epsilon = \frac{k_B T}{aD^2}, \quad \delta_k = \frac{a}{\gamma u_k^0}, \quad \rho_k = \frac{w_k^0}{u_k^0}. \quad (10)$$

Finally, if we assume a biphasic form for the elastic profile of the tail domain, then we can write

$$F(x-y) = a(x-y) + (b(x-y))^P,$$

and this nondimensionalization gives

$$\phi(z) = z + Cz^P,$$

where

$$C = b^P D^{P-1} a^{-1}.$$

Since the process above is translation-invariant, let us simplify by choosing $x = 0$ in what follows. Assume that we have a process such that some specified event occurs at a rate $R(y)$ (by which we mean specifically that in any given small time Δt the probability of occurrence of this event is given by $R(y)\Delta t$) and that y evolves according to $\dot{y} = \delta\phi(y)$, with $\phi(y) > 0$ for all $y > 0$ and $\phi(y) < 0$ for $y < 0$. We also assume that $R(y)$ scales as $R(y) = \exp(\psi(y)/\epsilon)$. We want to compute, given $y_I < y_F < 0$, the probability of the event occurring before $y = y_F$ if we start the process at $y = y_I$. We denote this probability as $P(y_I, y_F)$. By definition,

$$\frac{d}{dt}P(y_I, y(t)) = R(y(t))(1 - P(y_I, y(t))), \quad (11)$$

and using the differential equation for y we can write this as

$$\frac{d}{dy}P(y_I, y) = \delta^{-1}\frac{R(y)}{\phi(y)}(1 - P(y_I, y)). \quad (12)$$

We can solve Eq. 12 to obtain

$$P(y_I, y_F) = 1 - \exp\left(-\int_{y_I}^{y_F} \frac{\delta^{-1}R(y)}{\phi(y)}dy\right). \quad (13)$$

Writing $\delta^{-1} = \exp(\beta/\epsilon)$ and $R(y) = \exp(\rho(y)/\epsilon)$ gives

$$P(y_I, y_F) = 1 - \exp\left(-\int_{y_I}^{y_F} \frac{\exp(\epsilon^{-1}(\rho(y) + \beta))}{\phi(y)}dy\right). \quad (14)$$

We first consider the limit $\epsilon \to 0$. If there are any $y \in (y_I, y_F)$ for which $\rho(y) + \beta > 0$, the innermost exponential is exponentially large, and $P(y_I, y_F)$ is exponentially close to one. Similarly, if it is true that $\phi(z) + \beta < 0$ for all $y \in (y_I, y_F)$, the integral is exponentially small, and $P(y_I, y_F)$ is exponentially close to zero.

Now we compute the moments of y_F. Assume that we are in state S_k with the motor located at x_k, then the forward rate is

$$u_k(y) = \exp(-\theta_k^+ \phi(x_k - y)/\epsilon).$$

The evolution of y is given as $\dot{y} = \delta_k\phi(y)$. We define y_k^R to be the (unique) solution to $-\theta_k^+\phi(x_k - y) + \beta_k = 0$, where we define

$$\beta_k = \epsilon \log \delta_k^{-1}. \quad (15)$$

Then from the above argument, if we start the system at $y_I < y_k^R$, then

$$\lim_{\epsilon\to 0} P(y_I, y_F) = \begin{cases} 0, & y_F < y_k^R, \\ 1, & y_F > y_k^R. \end{cases} \quad (16)$$

This is because the function $-\theta_k^+\phi(x_k - y) + \beta_k$ is an increasing function of y, is negative for all $y < y_k^R$, and is positive for all $y > y_k^R$. The correct interpretation of this is that in the limit $\epsilon \to 0$, the system jumps perfectly reliably at the point $y = y_k^R$; in other words, if we start the system with any initial separation $> y_k^R$, then the probability of it having jumped before the separation reaches y_k^R is zero, but the probability of it jumping after the separation passes y_k^R, is one.

Of course, for any ϵ positive but small, $P(y_I, y_F)$ is a smooth function of y_I and y_F, so that instead of having a discontinuity at y_k^R, the function moves smoothly, but rapidly, from 0 to 1 as y_F decreases from y_I to 0.

To compute the moments of y_F, the authors performed an asymptotic analysis (see (51) and R. E. L. DeVille, C. B. Muratov, and E. Vanden-Eijnden, unpublished, for more detail) of a boundary layer expansion in the cumulative distribution function Eq. 14 in the limit $\epsilon \to 0$. It is shown that this function has a boundary layer of width $O(\epsilon)$, and that one can compute the moments of when the motor will jump (the probability distribution function of the location of the jump is $\partial P/\partial y_F$). The result of the calculation is that if we choose the initial separation between motor and cargo sufficiently $< z$, and let y_F be the random variable denoting where the motor first jumps forward, then

$$\langle y_F \rangle = y_k^R - \epsilon\left(\frac{\log\left(\frac{\phi'(y_k^R)}{\phi(y_k^R)e^{\tilde{\gamma}}}\right) + \log\epsilon}{\phi'(y_k^R)}\right) + O(\epsilon^2)$$
$$\langle (y_F - \langle y_F \rangle)^2 \rangle = \frac{\epsilon\pi^2}{6(\phi'(y_k^R))^2} + O(\epsilon^2), \quad (17)$$

where $\tilde{\gamma}$ is the Euler-Mascheroni constant

$$\tilde{\gamma} = \lim_{n\to\infty}\left(\sum_{k=1}^{n}\frac{1}{k} - \log n\right) \approx 0.5772.$$

Thus as we let $\epsilon \to 0$, the variance of the separation at jump goes to zero, meaning that the position of the jump becomes reliable. In fact, this analysis allowed one to compute all of the moments (asymptotically in ϵ, of course) of y_F in a similar manner, but here we only need to show that the variance goes to zero in ϵ.

Numerical details corresponding to myosin-V

A choice of β_j determines the asymptotic expansion in ϵ: setting β_j determines y_j^R, and then in Eq. 17 this determines the moments of y_F. To determine the dynamics of the system and how it depends on parameters, one need only determine the dependence of the β_j values on parameters. We point out that for the specific case of myosin-V, the two parameters β_0, β_1 can be modulated independently by varying γ and [ATP].

We claim that the dominating effect is the nonlinearity in the elastic profile of the tail domain. If we choose $\gamma = 10^{-4}\,\mathrm{kg\,s^{-1}}$ and [ATP] = 2 mM, then we have

$$\delta_0 = 3.57\times10^{-5}, \quad \delta_1 = 4.17\times10^{-3}, \quad \beta_0 = 6.321, \quad \beta_1 = 3.383.$$

This gives

$$\phi(y_0^R) \approx 632.1, \quad \phi(y_1^R) \approx 75.24, \quad y_0^R \approx -1.868, \quad y_1^R \approx -1.411.$$

(Recall that these are in nondimensional units where the scaling is the period of the motor, namely $D = 36$ nm, so these correspond to the physical distances of 67.26 nm and 50.80 nm.) In particular, this gives

$$\phi'(y_0^R) \approx 202, \quad \phi'(y_1^R) \approx 17.1.$$

On the other hand, the nondimensional parameter ϵ is not small for myosin-V (in fact, it is ~0.618). Thus, the motor is operating in the regime where the nonlinearity in the elastic profile of the tail domain is dominant; this is the effect which, for myosin-V, makes the variance in the period small.

Motor steady-state computation

Fix the position of the cargo at some y. We assume throughout this analysis that the cargo is moving so slowly that the motor has time to oscillate among several sites. The motor transitions between the states x_k such that it moves forward with rate $u_k(y)$ and backward with rate $w_k(y)$. If the cargo is fixed at y for a long period, then the position of the motor will satisfy the steady-state distribution $\pi(y)$, which solves

$$\pi_{k+1}(y)w_{k+1}(y) = \pi_k(y)u_k(y), \quad \sum_k \pi_k(y) = 1. \tag{18}$$

To be more specific, if this $\pi(y)$ exists and is unique, then we expect to find the motor at site x_k with probability $\pi_k(y)$ when the cargo is held fixed at y. (We set u_k, w_k to u_0, w_0 whenever k is even and u_1, w_1 whenever k is odd, since after two steps forward the motor ends up in the same state.) To compute this numerically, we can use the recursion equation (Eq. 18) to obtain the following scheme: Choose $m_0(y) = 1$, then compute

$$m_k(y) = \frac{\prod_{i=0}^{k-1} u_i(y)}{\prod_{i=1}^{k} w_i(y)}, \tag{19}$$

and then

$$\pi_k(y) = \frac{m_k(y)}{\sum_k m_k(y)}. \tag{20}$$

This gives a unique answer, as long as $\sum_k m_k(y) < \infty$. Notice, however, that in any model of the form Eq. 1, $u_k(y)/w_{k+1}(y) \to 0$ is exponentially fast, so this sum will be finite. More generally, in any model where backward stepping becomes very probable for long extensions of the tail, we will obtain a well-defined and unique steady state.

The authors thank Paul Atzberger, George Oster, and Charles Peskin for illuminating discussions regarding this work.

R.E.L.D. was supported as a Courant Instructor during some of this work. The work of E.V.-E. was partially supported by the National Science Foundation via grant No. DMS02-39625, and by the U.S. Office of Naval Research via grant No. N00014-04-1-0565.

REFERENCES

1. Alberts, B., A. Johnson, J. Lewis, M. Raff, K. Roberts, and P. Walter. 2002. Molecular Biology of the Cell, 4th Ed. Garland Science, New York.
2. Howard, J. 2001. Mechanics of Motor Proteins and the Cytoskeleton. Sinauer Associates, Sunderland, MA.
3. Lodish, H., A. Berk, P. Matsudaira, C. A. Kaiser, M. Krieger, M. P. Scott, L. Zipursky, and J. Darnell. 2003. Molecular Cell Biology, 5th Ed. W. H. Freeman, New York.
4. Rice, S., A. W. Lin, D. Safer, C. L. Hart, N. Naber, B. O. Carragher, S. M. Cain, E. Pechatnikova, E. M. Wilson-Kubalek, M. Whittaker, E. Pate, R. Cooke, E. W. Taylor, R. A. Milligan, and R. D. Vale. 1999. A structural change in the kinesin motor protein that drives motility. *Nature*. 402:778–784.
5. Visscher, K., M. J. Schnitzer, and S. M. Block. 1999. Single kinesin molecules studied with a molecular force clamp. *Nature*. 400:184–189.
6. Rief, M., R. S. Rock, A. D. Mehta, M. S. Mooseker, R. E. Cheney, and J. A. Spudich. 2000. Myosin-V stepping kinetics: a molecular model for processivity. *Proc. Natl. Acad. Sci. USA*. 97:9482–9486.
7. de la Cruz, E. M., E. M. Ostap, and H. L. Sweeney. 2001. Kinetic mechanism and regulation of myosin-VI. *J. Biol. Chem.* 276:32373–32381.
8. Mehta, A. D. 2001. Myosin learns to walk. *J. Cell Sci*. 114:1981–1998.
9. Rock, R. S., S. E. Rice, A. L. Wells, T. J. Purcell, J. A. Spudich, and H. L. Sweeney. 2001. Myosin-VI is a processive motor with a large step size. *Proc. Natl. Acad. Sci. USA*. 98:13655–13659.
10. Badoual, M., F. Julicher, and J. Prost. 2002. Bidirectional cooperative motion of molecular motors. *Proc. Natl. Acad. Sci. USA*. 99:6696–6701.
11. Lang, M. J., C. L. Asbury, J. W. Shaevitz, and S. M. Block. 2002. An automated two-dimensional optical force clamp for single molecule studies. *Biophys. J*. 83:491–501.
12. Veigel, C., F. Wang, M. L. Bartoo, J. R. Sellers, and J. E. Molloy. 2002. The gated gait of the processive molecular motor, myosin-V. *Nat. Cell Biol*. 4:59–65.
13. Block, S. M., C. L. Asbury, J. W. Shaevitz, and M. J. Lang. 2003. Probing the kinesin reaction cycle with a 2D optical force clamp. *Proc. Natl. Acad. Sci. USA*. 100:2351–2356.
14. Coureux, P.-D., A. L. Wells, J. Ménétrey, C. M. Yengo, C. A. Morris, H. L. Sweeney, and A. Houdusse. 2003. A structural state of the myosin V motor without bound nucleotide. *Nature*. 425:419–423.
15. Yildiz, A., J. N. Forkey, S. A. McKinney, T. Ha, Y. E. Goldman, and P. R. Selvin. 2003. Myosin-V walks hand-over-hand: single fluorophore imaging with 1.5-nm localization. *Science*. 300:2061–2065.
16. Yildiz, A., M. Tomishige, R. D. Vale, and P. R. Selvin. 2004. Kinesin walks hand-over-hand. *Science*. 303:676–678.
17. Thirumurugan, K., T. Sakamoto, J. A. Hammer III, J. R. Sellers, and P. J. Knight. 2006. The cargo-binding domain regulates structure and activity of myosin 5. *Nature*. 442:212–215.

18. Capitanio, M., R. Cicchi, and F. S. Pavone. 2007. Continuous and time-shared multiple optical tweezers for the study of single motor proteins. *Opt. Lasers Eng.* 45:450–457.

19. Uemura, S., H. Higuchi, A. O. Olivares, E. M. D. L. Cruz, and S. Ishiwata. 2004. Mechanochemical coupling of two substeps in a single myosin V motor. *Nat. Struct. Mol. Biol.* 11:877–883.

20. Shiroguchi, K., and K. Kinosita. 2007. Myosin V walks by lever action and Brownian motion. *Science.* 316:1208–1212.

21. Simon, S. M., C. S. Peskin, and G. F. Oster. 1992. What drives the translocation of proteins? *Proc. Natl. Acad. Sci. USA.* 89:3770–3774.

22. Leibler, S., and D. A. Huse. 1993. Porters versus Rowers—a unified stochastic-model of motor proteins. *J. Cell Biol.* 121:1357–1368.

23. Peskin, C. S., G. M. Odell, and G. F. Oster. 1993. Cellular motions and thermal fluctuations—the Brownian ratchet. *Biophys. J.* 65:316–334.

24. Peskin, C. S., and G. F. Oster. 1995. Coordinated hydrolysis explains the mechanical-behavior of kinesin. *Biophys. J.* 68:S202–S211.

25. Wang, H., T. Elston, A. Mogilner, and G. F. Oster. 1997. Force generation in RNA polymerase. *Biophys. J.* 74:1186–1202.

26. Astumian, R. D., and I. Derenyi. 1998. Fluctuation driven transport and models of molecular motors and pumps. *Eur. Biophys. J. Biophys. Lett.* 27:474–489.

27. Fisher, M. E., and A. B. Kolomeisky. 1999. The force exerted by a molecular motor. *Proc. Natl. Acad. Sci. USA.* 96:6597–6601.

28. Brady, S. T. 2000. Neurofilaments run sprints not marathons. *Nat. Cell Biol.* 2:E43–E45.

29. Elston, T. C., and C. S. Peskin. 2000. The role of protein flexibility in molecular motor function: coupled diffusion in a titled periodic potential. *SIAM J. Appl. Math.* 60:842–867.

30. Fisher, M. E., and A. B. Kolomeisky. 2001. Simple mechanochemistry describes the dynamics of kinesin molecules. *Proc. Natl. Acad. Sci. USA.* 98:7748–7753.

31. Mogilner, A., A. J. Fisher, and R. J. Baskin. 2001. Structural changes in the neck linker of kinesin explain the load dependence of the motor's mechanical cycle. *J. Theor. Biol.* 211:143–157.

32. Reimann, P. 2002. Brownian motors: noisy transport far from equilibrium. *Phys. Rep.* 361:57–265.

33. Kolomeisky, A. B., and M. E. Fisher. 2003. A simple kinetic model describes the processivity of myosin-V. *Biophys. J.* 84:1642–1650.

34. Atzberger, P. J., and C. S. Peskin. 2006. A Brownian dynamics model of kinesin in three dimensions incorporating the force-extension profile of the coiled-coil cargo tether. *Bull. Math. Biol.* 68:131–160.

35. Wang, H. 2006. A robust mathematical formulation for studying elastically coupled motor-cargo systems. *J. Comput. Theor. Nanosci.* 3:922–932.

36. Kolomeisky, A. B., and M. E. Fisher. 2007. Molecular motors: a theorist's perspective. *Annu. Rev. Phys. Chem.* 58:675–695.

37. Tsygankov, D., and M. E. Fisher. 2008. Kinetic models for mechanoenzymes: structural aspects under large loads. *J. Chem. Phys.* 128: 015102.

38. Schilstra, M. J., and S. R. Martin. 2006. Viscous load imposes a regular gait on myosin-V. *J. Roy. Soc. Interf.* 3:153–165.

39. DeVille, R. E. L., and E. Vanden-Eijnden. 2008. Regularity and synchrony in motor proteins. *Bull. Math. Biol.* 70:484–516.

40. Bustamante, C., J. F. Marko, E. D. Siggia, and S. Smith. 1994. Entropic elasticity of λ-phage DNA. *Science.* 265:1599–1600.

41. Rief, M., J. M. Fernandez, and H. E. Gaub. 1998. Elastically coupled two-level systems as a model for biopolymer extensibility. *Phys. Rev. Lett.* 81:4764–4767.

42. Schwaiger, I., C. Sattler, D. R. Hostetter, and M. Rief. 2002. The myosin coiled-coil is a truly elastic protein structure. *Nat. Mater.* 1: 232–235.

43. Muratov, C. B., E. Vanden-Eijnden, and E. Weinan. 2005. Self-induced stochastic resonance in excitable systems. *Physica D.* 210:227–240.

44. Freidlin, M. I. 2001. On stochastic perturbations of dynamical systems with fast and slow components. *Stoch. Dyn.* 1:261–281.

45. Berglund, N., and B. Gentz. 2006. Noise-induced phenomena in slow-fast dynamical systems: a sample-paths approach. *In* Probability and its Applications. Springer-Verlag London, London, New York.

46. DeVille, R. E. L., C. B. Muratov, and E. Vanden-Eijnden. 2005. Two distinct mechanisms of coherence in randomly perturbed dynamical systems. *Phys. Rev. E Stat. Nonlin. Soft Matter Phys.* 72:031105.

47. Gribble, F. M., G. Loussouarn, S. J. Tucker, C. Zhao, C. G. Nichols, and F. M. Ashcroft. 2000. A novel method for measurement of submembrane ATP concentration. *J. Biol. Chem.* 275:30046–30049.

48. DeVille, R. E. L., and E. Vanden-Eijnden. 2007. Self-induced stochastic resonance for Brownian ratchets under load. *Commun. Math. Sci.* 5:431–446.

49. Duke, T. A. J. 1999. Molecular model of muscle contraction. *Proc. Natl. Acad. Sci. USA.* 96:2770–2775.

50. Endow, S. A., and H. Higuchi. 2000. A mutant of the motor protein kinesin that moves in both directions on microtubules. *Nature.* 406:913–916.

51. DeVille, R. E. L., C. B. Muratov, and E. Vanden-Eijnden. 2005. Non-mean-field deterministic limits in chemical reaction kinetics far from equilibrium. *J. Chem. Phys.* 124:Article No. 231102.

52. Reference deleted in proof.